

# Synergistic Effect between Zinc Particles and Graphene on the Anti-Corrosion Performance of Epoxy Coatings

Jintao Zhang, Hu Wang\*, Juan Xie\*\*

School of New Energy and Materials, Southwest Petroleum University, Chengdu 610500, China

\*E-mail: [senty78@126.com](mailto:senty78@126.com) (Hu Wang), [jennyx99@126.com](mailto:jennyx99@126.com) (Juan Xie)

Received: 25 September 2022 / Accepted: 26 October 2022 / Published: 30 November 2022

In this paper, the synergistic effect between zinc particle and graphene as anti-corrosion coatings was investigated. The epoxy coatings with 0.5% graphene and different contents of zinc particles were prepared. The graphene was characterized by Raman and FT-IR spectra. Synergistic effect between different zinc content and graphene on the corrosion protection behaviors of epoxy coatings was examined by electrochemical impedance spectroscopy (EIS), salt spray and contact angle measurements. The results showed that the addition of 0.50% graphene into the coating could significantly enhance barrier effect of epoxy coating and reduce the amount of zinc powder in the zinc rich coating. The cross-sectional morphologies and elemental distribution of the 50 % Zn+0.50 % Gnps coating at different immersion time were analyzed by Scanning electron microscopy (SEM) and energy dispersive spectroscopy (EDS). The results confirmed that the zinc particles near the metal substrate have not significantly reduced in the early stage, indicating the metal has not undergone a severe corrosion. With the immersion time prolonged, the cross-section of the coating became uneven (after 20 days' immersion), which could be ascribed to the consumption of zinc particles in the coating.

**Keywords:** Epoxy coating; Graphene; Zinc particles; Synergistic effect; Electrochemical impedance spectroscopy

## 1. INTRODUCTION

Corrosion of metals has always been one of the most severe challenges in all industries. Not only does it cause great economic loss and energy waste, but also has many potential dangers. Among many anti-corrosion measures, utilizing coatings is a major approach for protecting steel away from corrosion attack [1-3]. The physical shielding effect of the neat epoxy resins can prevent coatings from corrosion. Once penetrated, the barrier property of the coating will be greatly weakened [4,5].

To compensate for the defects of epoxy resin, researchers introduced zinc particles to the coating. Compared with the potential of iron (-0.440 V vs. SCE), zinc (-0.762 V vs. SCE) has a remarkable

negative potential. Therefore, the zinc-rich epoxy coating not only possesses the physical shielding effect of conventional coating, but also zinc sacrificial anode is identified to provide an excellent electrochemical protection the metal due to a large amount of zinc powders exists in the coating [6]. In addition, the corrosion products of zinc can fill the holes of coating by forming a passivation layer [7]. In order to utilize the electrochemical cathodic protection of zinc-rich epoxy coating, effective electrical contact must be formed among the zinc particles and between the zinc powders and metal substrate in the coating. Generally, the zinc powder content in the coating is required to be more than 80% [8]. However, the high content of zinc powder will increase the porosity of the coatings, and damage the spraying ability and leveling property [9-11]. It has been reported that the concentration of zinc powder can be reduced and the cathodic protection time of zinc-rich coating can be prolonged by adding conductive fillers, such as carbon black [12], carbon fiber [13], polyaniline [14], and so on.

Graphene is considered as an excellent anti-corrosion material due to its two-dimensional nanostructure and unique properties, which has made a unprecedented progress in promoting the preparation of novel anti-corrosion coatings [15]. Adding graphene can prolong the cathodic protection time of the zinc-rich coating. Moreover, a galvanic cell can be formed between the zinc particles and the steel substrate even with low zinc contents [16], and once penetrated, the impermeability of graphene can extend the diffusion path of the aggressive species to the metal substrate [17]. Yang et al [18]. explored the optimum corrosion resistance performance by adding different contents of graphene. It concluded that the coating with the addition of 2.0 wt% graphene possessed the best anti-corrosion performance when the coating contained 40 wt% of zinc particles. Liu et al [19]. found that the coating with the addition of 0.6 wt% graphene showed the best anti-corrosion performance when the coating contained 80 wt% of zinc particles. Kong et al [20]. revealed the effect of different contents of graphene on the corrosion evolution of zinc particles in the waterborne zinc-rich epoxy coating. To date, the optimal content of graphene and zinc in composite coatings is unknown, and the corrosion evolution process of zinc particles in the coatings with different zinc contents is unclear.

In this work, 0.50 wt% graphene (Gnps) was added to epoxy coating. The coatings with different zinc contents, in the presence of Gnps, were prepared and the anti-corrosion performance was investigated by electrochemical measurements, salt spray test and surface analysis like contact angle, SEM and EDS.

## 2. EXPERIMENTAL DETAILS

### 2.1. Experimental materials

The tin plate sheets (from Guangzhou Honghong Industry Co., Ltd) with dimensions of 150×70×0.25 mm and the nominal chemical composition (wt%) of C 0.02, Mn 0.13, P 0.009, S 0.006 and Fe balance. Epoxy resin (E-51) and zinc-rich primer were purchased from Shanghai Wangqi Industry Co., Ltd. Zinc-rich primer composed of epoxy resin (E-51) and polyamide curing agent. Three different zinc-rich epoxy primers contained 30 wt%, 50 wt%, and 80 wt% of zinc particles, respectively. Graphene

was made in laboratory [21,23]. Xylene was purchased from Chengdu Kelong Chemical Reagent Co., Ltd.

## 2.2. Fabrication of coating samples

The composite coatings with the addition of 0.50 wt% Gnps nanosheets were prepared as follows: 0.05 g Gnps nanosheets were first placed in 2 g xylene and ultrasonicated for 30 min to obtain a homogeneous solution. Subsequently, 10 g E51/Zinc-rich epoxy resin was mixed into the prepared solution. Then the mixture was ultrasonicated for 5 min to acquire a uniform solution. A stoichiometric amount of polyamide curing agent was added to the uniform solution with a weight ratio of 2.5: 1 (epoxy resin: polyamide curing agent), and the mixture was stirred for 10 min. The carbon steel substrate was mechanically polished using 400, 800 and 1200-grit abrasive SiC to remove traces of surface oxide. After cleaned by distilled water, the metal substrate is further washed with ethanol. Finally, the prepare paints were applied on the surface of the carbon steel substrate by using a wire bar coater with a thickness of  $100 \pm 5 \mu\text{m}$ , and the coatings were cured at the ambient temperature for 48 h. The coatings with different zinc content were denoted as E51+0.50 % Gnps, 30 % Zn+0.50 % Gnps, 50 % Zn+0.50 % Gnps, 80 % Zn+0.50 % Gnps, respectively.

## 2.3. Characterization

Raman spectrum (Raman, Thermo Dxr2xi) and Fourier transform infrared spectrometer (FT-IR, WQF-520) were used to characterize graphene. The scanning electron microscopy (SEM, ZEISS EVO MA15) was utilized to observe the cross-sectional images of the composite coatings. The elemental composition was obtained through coupled Energy Dispersive X-ray Spectroscopy. In addition, the conductivity of graphene was measured by using a four-probe method.

## 2.4. Electrochemical measurements

The electrochemical measurements were conducted via an electrochemical workstation (CS310H, Wuhan Corrtest). A standard three-electrode cell was used as electrochemical measurement system at ambient condition, where the tin plate sheet with coatings was used as the working electrode, saturated Ag/AgCl electrode was used as reference electrode and a Pt electrode was used as counter electrode. The acrylic cylinder was fixed on the surface of the coating by adhesive sealant and the 80 % volume of the cylinder was occupied by 3.5 wt% NaCl solution. The immersion area of the coating is  $7 \text{ cm}^2$ . When conducting electrochemical tests, the working and counter electrode were immersed in NaCl solution for 10 min to attain a steady open-circuit potential (OCP). Then the EIS measurements were carried out with the frequency range of 100 KHz to 10 mHz with an amplitude of 10 mV. Furthermore, Zview2 software was used for fitting the EIS results. According to GB /T 1771-2007 [24], the neutral salt spray test was conducted in a chamber (Hangzhou Wujia mechanical equipment Co., Ltd) with

continuous spray at 35°C. In addition, the contact angle meter was utilized to record the variation in the water contact angle on the surface of the composite coatings before and after salt spray test.

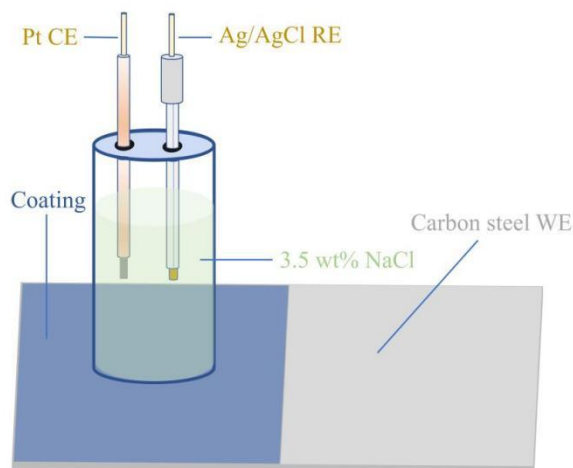


**Figure 1.** Schematic diagram of electrochemical measurements for coatings immersed in solution from 2 days to 70 days.

### 3. RESULTS AND DISCUSSION

#### 3.1. Characterization of graphene nanosheet

Raman spectra were performed to determine the chemical structure of prepared Gnps, as shown in Fig. 2a. The peaks at  $1342.7\text{ cm}^{-1}$ ,  $1576.1\text{ cm}^{-1}$  and  $2688.6\text{ cm}^{-1}$  correspond to D, G and 2D bands, respectively.

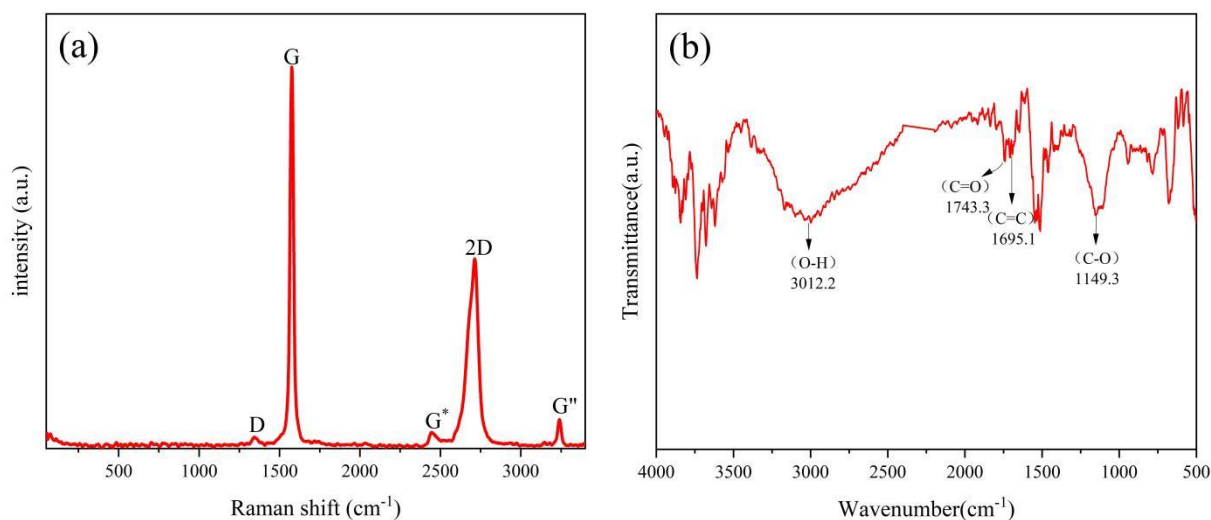


**Figure 2.** Characterization of prepared graphene. (a) Raman spectrum and (b) FT-IR spectrum.

D band represents defects and disorder of the sample. G band represents the crystallinity of the sample [5]. The 2D peak is associated with the resonant effect of the D band originating from the phonon dispersion process [25,26]. The small D peak indicates that the Gnps is close to the pristine state with only a few defects. The peak at  $2447.7\text{ cm}^{-1}$  and  $3240.3\text{ cm}^{-1}$  corresponds to  $G^*$  and  $G''$ , respectively. The  $G^*$  and  $G''$  bands are defects activated bands [25]. The chemical bonding of Gnps was characterized through FT-IR in Fig. 2b. The characteristic absorption peak at  $3012.2\text{ cm}^{-1}$  corresponds to the stretching vibration of O-H [27]. The peaks at  $1149.3\text{ cm}^{-1}$ ,  $1695.1\text{ cm}^{-1}$  and  $1743.3\text{ cm}^{-1}$  correspond to C-O, C=C and C=O [28], respectively. The conductivity of Gnps after tableting was  $971\text{ S/cm}$ . The prepared Gnps has high electrical conductivity [27,29], which can provide better electrical conductivity and enhance the cathodic protection ability of the coatings.

### 3.2. EIS measurement

#### 3.2.1. E51/E51+0.50 % Gnps

The protection of metal originates from the shielding effect of E51 and E51+0.50 % Gnps coating. As shown in Fig. 3a, the Nyquist plots of the E51 coating showed two capacitive arcs during the whole immersion period [14]. The capacitive arc in the high frequency region corresponds to the shielding effect of the coating from corrosive media and the arc at low-frequency region was associated with corrosion process [30,31]. The capacitive arcs became smaller when the immersion time from 2 days to 8 days. Shen et al proved that this phenomenon was related to a prominent deterioration of the coating after absorbing large amounts of water [5]. Generally, the barrier performance of the coatings could be evaluated according to the impedance modulus at the lowest frequency ( $|Z|_{0.01\text{Hz}}$ ), and a higher value means better corrosion resistance [13]. The semicircle in the high frequency region became larger when the immersion time from 14 days prolonged to 20 days, the corresponding  $|Z|_{0.01\text{Hz}}$  value slightly increased from  $3798.4\ \Omega\ \text{cm}^2$  (14 days) to  $4751.5\ \Omega\ \text{cm}^2$  after 20 days immersion. This phenomenon might be related to the formation of corrosion products, which could prevent metal base from further corrosion. [32, 33]. In the phase angle plots, two time constants could be observed in Fig. 3c during the whole immersion test. With longer exposure time, the peak height decreased gradually and eventually became a straight line in low-frequency region after 70 days of immersion. This behavior is related to the increase of corrosion products in coating and reduced the migration rate of mass, which became the control step of corrosion reaction [18].

In case of E51+0.50 % Gnps coating, only one capacitive arc appeared by introducing Gnps after 2 days of immersion seen from Fig. 3d, meant the corrosive media had not reached the metal substrate. It can be attributed to the physical shielding effect of Gnps, which can extend the diffusion path of the corrosive media to the carbon steel substrate [34]. With the time progressed, Nyquist impedance plots evolved from one capacitive loop to three capacitive loops which indicated aggressive species had arrived the metal base and the corrosion product layer formed on the surface of the steel substrate [35]. As seen from Fig.3e, a line appeared in the middle frequency region from 40 days to 70 days, and the corresponding  $|Z|_{0.01\text{Hz}}$  value significantly decreased in Fig. 6b. This illustrated the barrier performance of the E51+0.50 % Gnps coating had been a sharp decline. The same as E51 coating, the  $|Z|_{0.01\text{Hz}}$  value

of the E51+0.50 % Gnps coating maintained relative stability due the corrosion products formed in the middle stage. In the phase angle plots, only one time constant could be observed at 2 days, suggested the coating had not been penetrated. Three time constant appeared after 5 days of immersion, the first time constant in the high frequency was related to the formation of corrosion products layer, the second time constant in the middle frequency is associated with the corrosion resistance ability of the coating and the third time constant in the low frequency represents the corrosion process [35,36], respectively. Compared with E51 coating, the E51+0.50 % Gnps coating exhibited a higher  $|Z|_{0.01\text{Hz}}$  value at different immersion time and just appeared one capacitive arc after 2 days immersion, suggested the improvement of barrier effect for the coating after adding 0.50 % Gnps [14].

To further characterize the corrosion behavior of different coatings, EIS data were fitted with equivalent circuit models (Fig.4) and the corresponding electrochemical parameters obtained from fitting were presented in Table 1. Among the models,  $R_s$ ,  $R_f$ ,  $R_{ct}$  represents the solution resistance, the resistance of the corrosion product layer and charge transfer resistance, respectively.  $C_f$ ,  $CPE_{dl}$  represents the corrosion product layer capacitance and the double-layer capacitance. The Warburg element (W) was related to diffusion behavior of the coatings. The value of CPE-P ( $n_{dl}$ ) represents different electrochemical behaviors [14]. The equivalent circuit model of the E51 coating from 2 days to 8 days was shown in Fig 4b. Introduced the Warburg component to the model due to the corrosion media had arrived the metal base after 2 days of immersion. Normally, The  $R_{ct}$  value is inversely proportional to the corrosion rate of the steel/coating interface. It's a basic parameter for evaluating the corrosion resistance performance of the coating. [28, 33]. As shown in Fig 4a, from 2 days to 8 days, the variation regulation of  $R_{ct}$  gradually declined for E51 coating, thereby manifested the degradation in anti-corrosion performance. However, the value of  $R_{ct}$  exhibited an increased trend from 8 days to 20 days, which was related to the formation of corrosive production layer [32]. Hence, the equivalent circuit model was shown in Fig 4c from the 14th day. The value of  $R_f$  increased slightly from  $80.35 \Omega \text{ cm}^2$  (14 days) to  $118.4 \Omega \text{ cm}^2$  after 20 days immersion in Table 1, the increased value indicated the accumulation of corrosion products and the difficulty in the penetration of the aggressive species through the corrosion product. The low  $R_f$  value ( $29.59 \Omega \text{ cm}^2$ ) was shown in Table 1 illustrated the corrosion products layer had been penetrated after 70 days immersion, and the E51 coating had completely failed [37]. The equivalent circuit model of E51+0.50 % Gnps coating was shown in Fig. 4a on the second day for immersion, suggested the corrosion media not penetrated the coating. With longer exposure time, three capacitive arcs appeared in Nyquist plots, and the corresponding model was shown in Fig. 4c, suggested the corrosion products formed after 5 days of immersion. Notably, the value of  $R_f$  continuous increased from  $62.65 \Omega \text{ cm}^2$  (5 days) to  $116.1 \Omega \text{ cm}^2$  (20 day) in Table 1 due to the accumulation of corrosion products. Furthermore, the  $R_f$  value gradually decreased to  $74.96 \Omega \text{ cm}^2$  after 70 days immersion which exhibited a higher  $R_f$  value compared with the E51 coating, indicated the slight penetration of the corrosion media through the corrosion product layer and a better barrier performance of corrosion products layer. A higher  $R_{ct}$  value could obtain from Table 1 for E51+0.50 % Gnps coating at different immersion time, it could be attributed to the barrier effect of Gnps. All equivalent circuit models and the corresponding fitting values indicated that the E51+0.50 % Gnps coating possessed a better anti-corrosion performance with the addition of 0.50 % Gnps and longer immersion time.

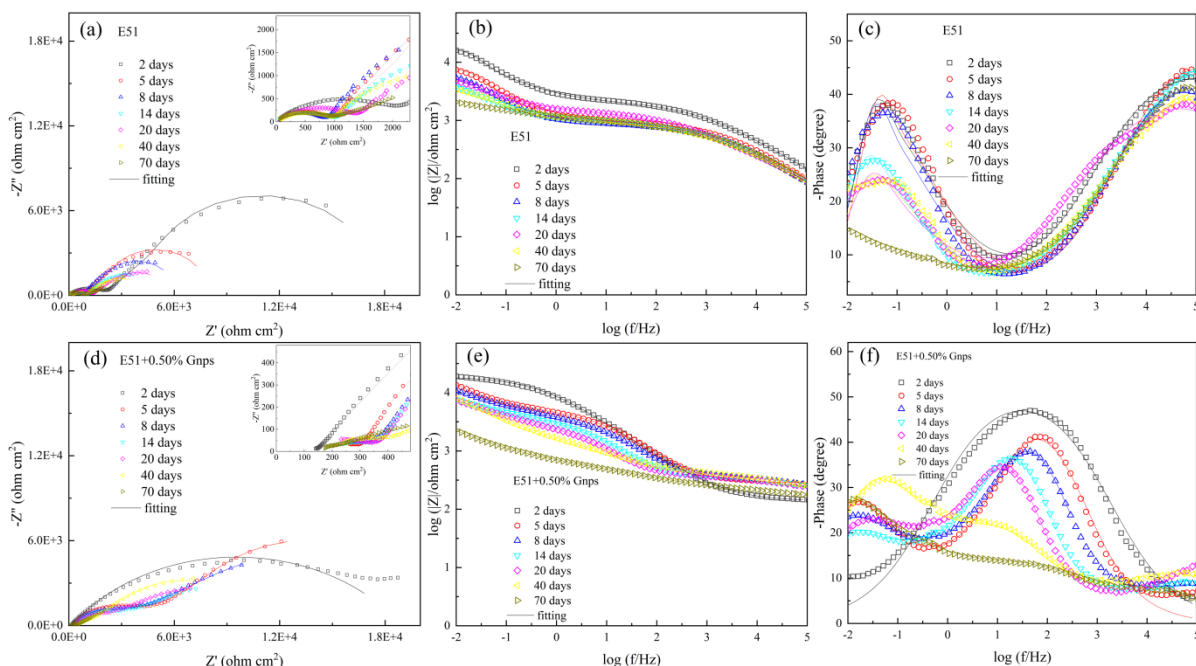


**Figure 3.** Nyquist and Bode plots of coating varied with immersion time. (a-c) E51, (d-f) E51+0.50 % Gnps.

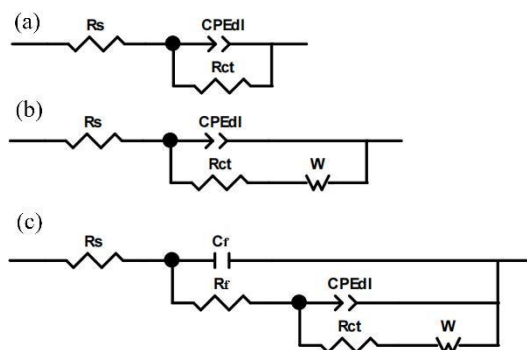


**Figure 4.** The equivalent circuit models utilized to fit the EIS data. (a) for the EIS on the second day of the E51+0.50 % Gnps coating, from 2 days to 8 days of the 80 % Zn+0.50 % Gnps coating, (b) for the EIS at most conditions excepted (a) and (c), (c) for the EIS from 14 days to 70 days of the E51 coating and from 5 days to 70 days of the E51 +0.50 % Gnps coating.

**Table 1.** Electrochemical parameters of the composite coatings by fitting.

Samples	Time (days)	$C_f (\Omega^{-1}S^{-n}cm^{-2})$	$R_f (\Omega cm^2)$	$CPE_{dl-T} (\Omega^{-1}S^{-n}cm^{-2})$	$CPE_{dl-P}$ or $n_{dl}$	$R_{ct} (\Omega cm^2)$	$R_w (\Omega cm^2)$
E51	2	---	---	$4.6775 \times 10^{-6}$	0.54	2055	15605
	5	---	---	$3.9382 \times 10^{-6}$	0.59	899	6942
	8	---	---	$4.9981 \times 10^{-6}$	0.58	785	5240
	14	$1.6863 \times 10^{-8}$	80.35	$1.1581 \times 10^{-5}$	0.53	847	3698
	20	$2.3079 \times 10^{-8}$	118.40	$1.0366 \times 10^{-5}$	0.57	1113	4565
	40	$2.0607 \times 10^{-8}$	105.10	$9.7316 \times 10^{-6}$	0.56	721	3567
	70	$1.2662 \times 10^{-8}$	29.59	$1.1944 \times 10^{-6}$	0.51	790	3245
	2	---	---	$2.5994 \times 10^{-5}$	0.60	18826	---
	5	$3.5825 \times 10^{-8}$	62.65	$1.1795 \times 10^{-5}$	0.73	3731	17630
	8	$5.6768 \times 10^{-8}$	96.98	$1.7080 \times 10^{-5}$	0.73	2745	17320

E51+0.50%Gn ps	14	$6.8593 \times 10^{-8}$	100.90	$3.2416 \times 10^{-5}$	0.72	2453	10225
	20	$4.6425 \times 10^{-8}$	116.10	$5.2326 \times 10^{-5}$	0.70	2115	8132
	40	$1.2396 \times 10^{-7}$	98.78	$1.6725 \times 10^{-4}$	0.49	1643	10638
	70	$1.0543 \times 10^{-7}$	74.96	$1.3085 \times 10^{-4}$	0.49	613.4	7504
	2	---	---	$3.9732 \times 10^{-7}$	0.83	10430	122980
30%Zn+0.50% Gnps	5	---	---	$1.3608 \times 10^{-7}$	0.87	5241	54232
	8	---	---	$5.2810 \times 10^{-7}$	0.67	4802	30987
	14	---	---	$4.4762 \times 10^{-7}$	0.77	3942	18664
	20	---	---	$1.8885 \times 10^{-6}$	0.61	3383	9183
	40	---	---	$6.4441 \times 10^{-6}$	0.53	1323	6381
	70	---	---	$6.0940 \times 10^{-6}$	0.53	1416	9618
	2	---	---	$2.1808 \times 10^{-7}$	0.60	678750	$7.7590 \times 1$
50%Zn+0.50% Gnps	5	---	---	$3.4269 \times 10^{-7}$	0.56	819300	$5.2052 \times 1$
	8	---	---	$2.1808 \times 10^{-7}$	0.60	678750	$1.4612 \times 1$
	14	---	---	$4.6167 \times 10^{-7}$	0.59	432440	856770
	20	---	---	$4.4123 \times 10^{-7}$	0.62	387500	860560
	40	---	---	$7.8904 \times 10^{-7}$	0.59	97512	500800
	70	---	---	$9.2639 \times 10^{-7}$	0.58	37308	76840
	2	---	---	$1.7940 \times 10^{-6}$	0.76	796080	---
80%Zn+0.50% Gnps	5	---	---	$1.5024 \times 10^{-6}$	0.81	471350	---
	8	---	---	$2.0695 \times 10^{-6}$	0.74	451140	---
	14	---	---	$3.7412 \times 10^{-6}$	0.65	86761	120500
	20	---	---	$4.7845 \times 10^{-6}$	0.61	33945	109310
	40	---	---	$7.0552 \times 10^{-6}$	0.55	3246	11578
	70	---	---	$1.6662 \times 10^{-6}$	0.78	1346	4198

### 3.2.2. Zn+0.50 % Gnps

By adding 30 %Zn to E51+0.50 % Gnps coating, not only does it possess physical barrier effect, but also has the capacity of cathodic protection [38]. As shown in Fig. 5a, one semicircle and straight line appeared in the high frequency and low frequency region after 2 days immersion, respectively. This phenomenon manifested the mass transfer process took a dominant position and the corrosion products lied on the surface of steel substrate at this time [18]. With 5 days exposure time, the line evolved into an arc at low-frequency region, suggested a charge transfer process of zinc particles existed at the interface of zinc/steel substrate [13]. Cao et al found that zinc content of at least 40 wt% is necessary to activate sacrificial protective effect on the steel substrate [39]. However, by introducing high conductivity Gnps to the 30 wt % zinc content coating, which could accelerate more zinc particles to be activated to provide cathodic protection on metal with the immersion time prolonged. The  $|Z|_{0.01\text{Hz}}$  value decreased slightly from 5 days to 14 days in Bode diagram, it could be attributed to cathodic protection in the early stage [13]. Compared with E51+0.50 % Gnps coating, a higher  $|Z|_{0.01\text{Hz}}$  value illustrated better barrier effect for 30 %Zn+0.50 % Gnps coating at most of the time. As seen from phase angle plots, two time constants appeared during the whole immersion procedure, manifested the defects of holes existed in the coating after adding 30 % Zn [9]. These defects allowed the diffusion of corrosive media, led to the corrosion of metal substrate [40]. With longer immersion time, the phase angle seen from Fig. 5 shifted towards higher frequency value stand for the zinc corrosion products formed between the surface of three different zinc content coating and corrosion solution, which further reduced the surface-active area and acted as barrier layer [35].

Nyquist plots of the 50 %Zn+0.50 % Gnps coating after 2days immersion were shown in Fig. 5d. A capacitive arc and small diffusion tail appeared at high-frequency and low-frequency region,

respectively, indicated the steel substrate has not undergone a large-scale corrosion process owe to excellent cathodic protection performance. After 5 days for immersion, a larger semicircle radius at high-frequency region could be observed, manifested Gnps on improving the electrical connectivity was more effective among 50 % content zinc particles. With longer immersion time, the coating possessed an excellent cathodic protection effect as more zinc particles been activated by Gnps [41]. The  $|Z|_{0.01\text{Hz}}$  value of 50 %Zn+0.50 % Gnps coating on the second day was  $9.42 \times 10^5 \Omega \text{ cm}^2$ , while the  $|Z|_{0.01\text{Hz}}$  value of 30 %Zn+0.50 % Gnps coating was  $5.92 \times 10^4 \Omega \text{ cm}^2$ , proved that 50 %Zn+0.50 % Gnps coating achieved better barrier effect than 30 %Zn+0.50 % Gnps coating.  $|Z|_{0.01\text{Hz}}$  value of 50 %Zn+0.50 % Gnps coating exhibited a significantly decreased trend from the 20th day, suggested cathodic protection began to fail. In addition, the 50 %Zn+0.50 % Gnps coating hadn't swelled or peeled off during the immersion test for 70 days, and the impedance spectrum test results also show that the coating did not enter the failure period, indicating that the coating still protects the substrate metal [42].

When the steel was coated with 80 %Zn+0.50 % Gnps coating, just one capacitive arc appeared in the Nyquist plots from 2 days to 8 days. This phenomenon indicated that the zinc corrosion products could fill the holes caused by adding zinc powder [43,44]. It's clear that the synergy effect between high content zinc and Gnps was more effective in the early stage. Another arc could be observed in the low-frequency region from the 14th day and  $|Z|_{0.01\text{Hz}}$  value decreased significantly from  $4.42 \times 10^5 \Omega \text{ cm}^2$  (8 days) to  $1.31 \times 10^5 \Omega \text{ cm}^2$  (14 days), manifested the coating had been penetrated and the cathodic protection began to fail. The  $|Z|_{0.01\text{Hz}}$  value held stability from 14 days to 20 days in Fig. 6b, it could be attributed to the barrier effect of corrosion product and Gnps. Compared with 50 %Zn+0.50 % Gnps coating, the 80 %Zn+0.50 % Gnps coating with a relatively lower  $|Z|_{0.01\text{Hz}}$  value and shorter cathodic protection time, suggested a large amount of zinc corrosion products wrapped up the surrounding unactivated zinc particles in the early stage and thus gradually failed to provide cathodic protection to metal [45].

The E51+0.50 % Gnps coating' model was presented in Fig. 4a after 2 days immersion, there was no Warburg element in the model. The equivalent circuit model for 30 % Zn+0.50 % Gnps and 50 % Zn+0.50 % Gnps coating was shown in Fig. 4b. The Warburg element of the model indicated the defects existed in the coating due to add Zinc particles. After 2 days immersion, the corrosive media had arrived at the metal base in the initial stage of immersion procedure. The  $R_{ct}$  values showed that even if there were defects in the coating, it still had a better protective effect to the metal base than E51/E51+0.50 % Gnps coating. Compared with other coatings, the 80 % Zn+0.50 % Gnps coating exhibited the highest  $R_{ct}$  value at 2 days in Table 1, indicated the 0.50 % Gnps had the most significant effect on the electrical connection of the high zinc content coating. The rest of the time, the anti-corrosion performance of 50 % Zn+0.50 % Gnps coating proved that achieved better behaviour than other coating samples. As the cathodic protection failed, the Gnps and zinc corrosion products acted as barrier layer could hold the anti-corrosion performance relative stability for a period of time. The  $R_{ct}$  value of 50 % Zn+0.50 % Gnps coating was relatively closed to 80 % Zn+0.50 % Gnps coating, this demonstrated the corrosion resistance performance of the coating was greatly improved by appropriately increasing the content of zinc powder in the presence of 0.50 % Gnps. Additionally, with the immersion time prolonged, it was found that the charge transfer resistance  $R_{ct}$  of all coating samples decreased in varying degrees. It means that the corrosion resistance of the coating decreases gradually [46-48].

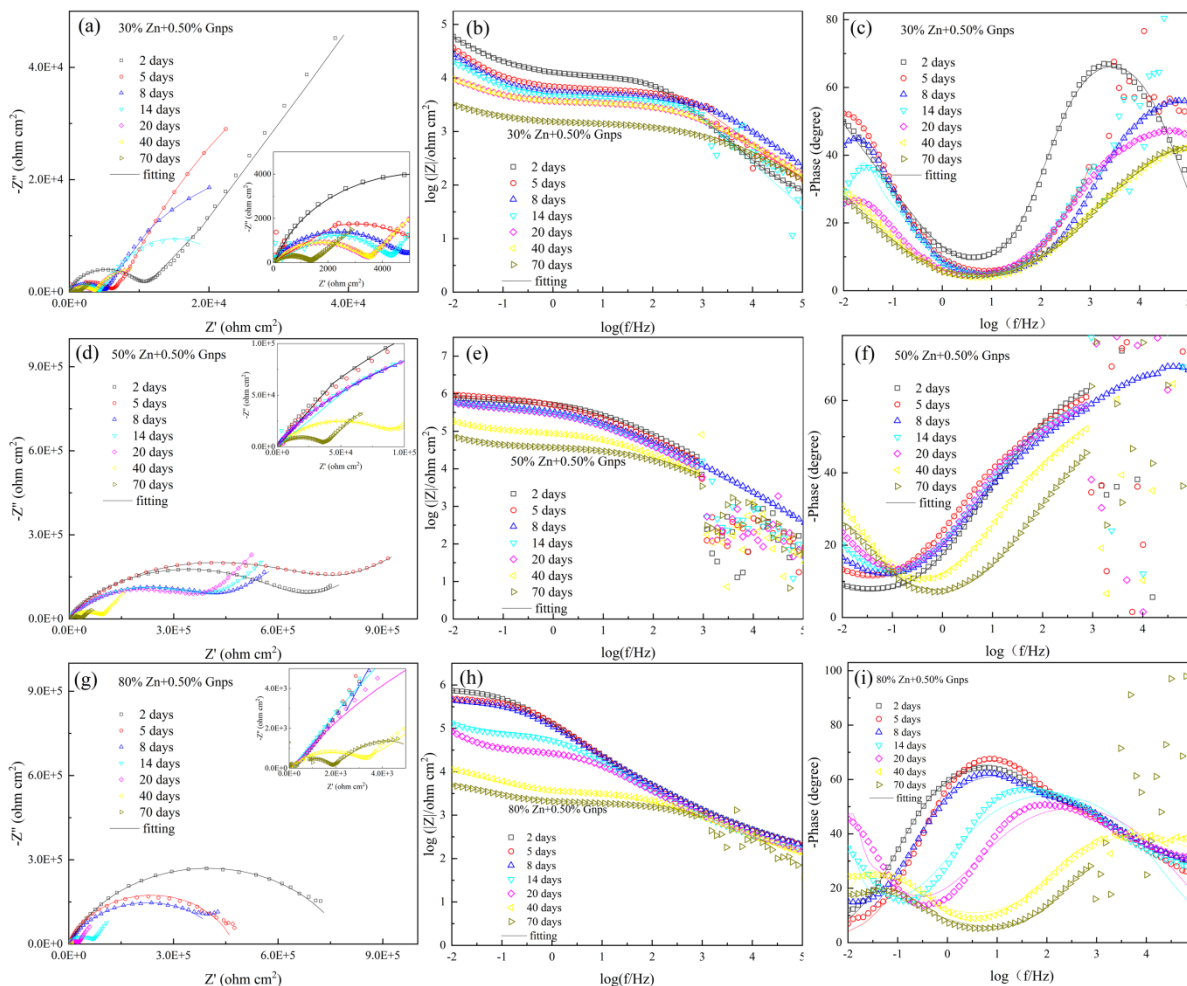


**Figure 5.** Nyquist and Bode plots of coating varied with immersion time. (a-c) 30 % Zn+0.50 % Gnps, (d-f) 50 % Zn+0.50 % Gnps, (g-i) 80 % Zn+0.50 % Gnps.

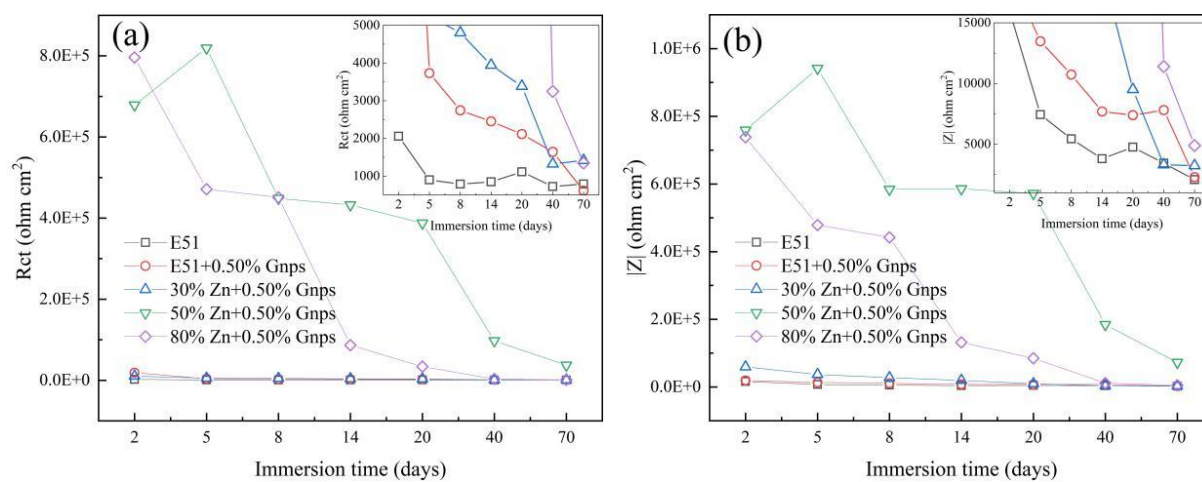


**Figure 6.** Variation trend of (a)  $R_{ct}$  and (b)  $|Z|_{0.01\text{Hz}}$  for all coatings over 70 days of immersion.

### 3.3. Morphologies of coatings

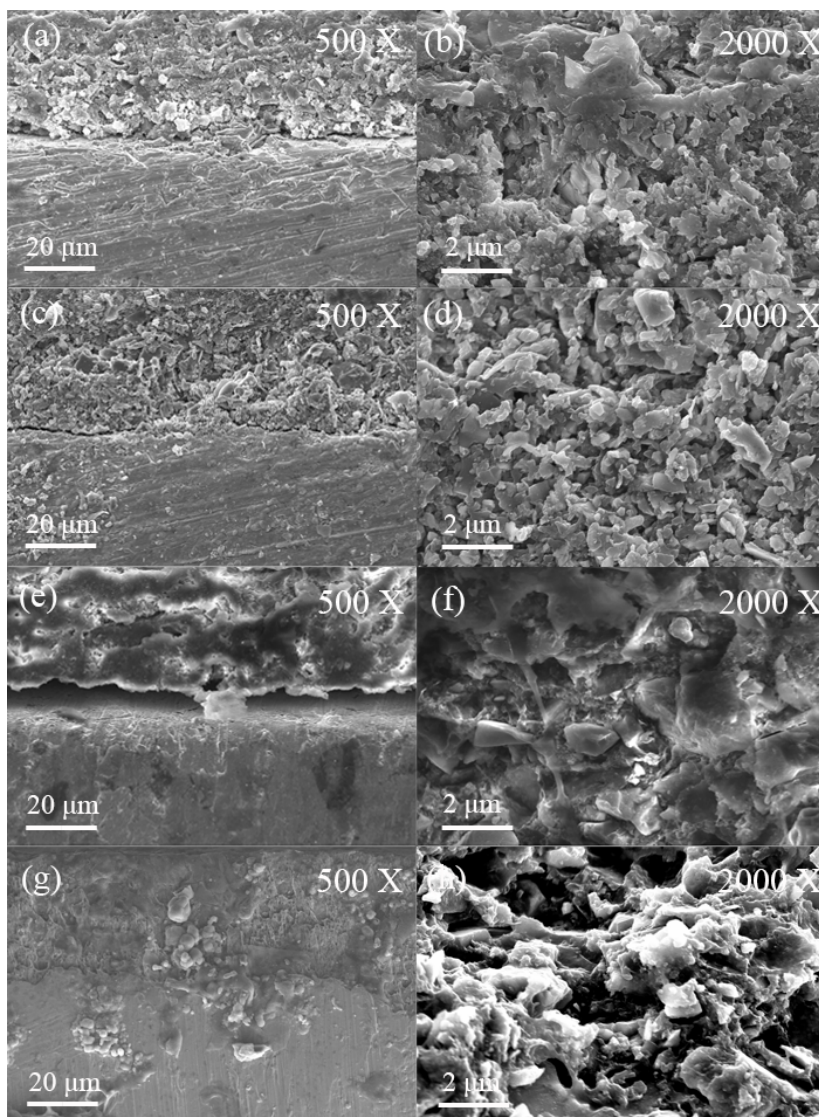


**Figure 7.** The cross-sectional images of the 50 % Zn+0.50 % Gnps coating under different immersion time in 3.5 wt% NaCl. (a, b) before immersion, (c, d) 2 days, (e, f) 20 days, (g, h) 70 days of immersion.

The cross-sectional morphologies of the 50 % Zn+0.50 % Gnps coating at different immersion time were shown in Fig. 7. The coating exhibits as compact before and after 2 days of immersion, no corrosion products were observed between coating and steel substrate which meant the steel substrate was protected by the coating during 2 days of immersion. Furthermore, it can be observed that the spherical zinc particles were uniformly dispersed and isolated with each other in the coatings. In order to improve the cathodic protection effect, introduced Gnps to enhance the electrical connection between zinc particles. As seen from Fig. 7e, delamination phenomenon appeared between coating and steel substrate after 20 days of immersion. The cross-sectional of the coating became uneven as shown in Fig. 7f, it was due to remaining holes formed after the zinc particles were consumed. Therefore, indicating a strong cathodic protection effect in the early stage accompanied the zinc particles were uniformly

corroded in the coatings. As shown in Fig. 7g, the corrosive media completely penetrated into the surface of the steel substrate after 70 days of immersion. The close combination at coating-metal interface could be observed, which can be attributed to the formation of corrosion products that filled the gaps between coating and metal. As mentioned, there were more holes could be observed as shown in Fig. 7h, meant the cathodic protection effect has completely failed.

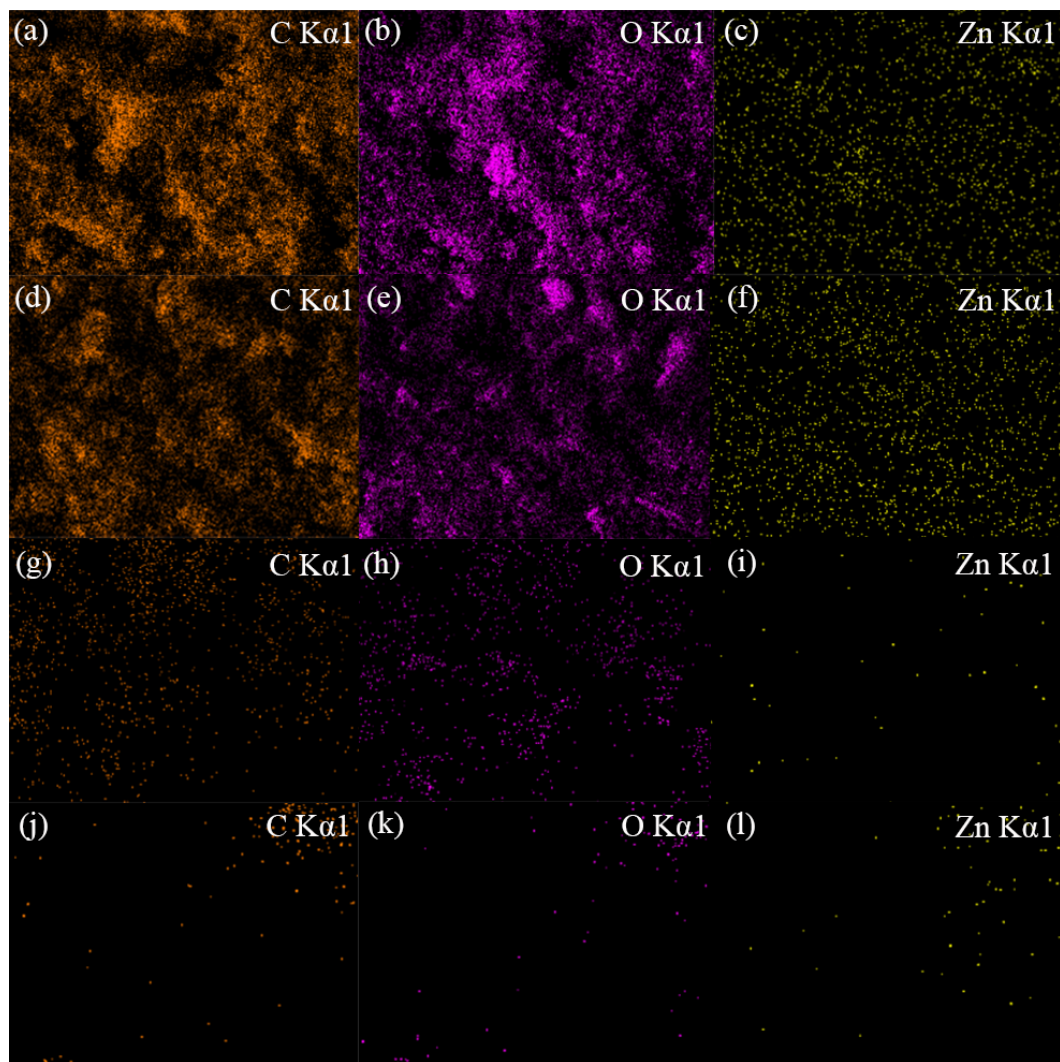


**Figure 8.** The EDS mapping and spectra for the 50 % Zn+0.50 % Gnps coating under different immersion time in 3.5 wt% NaCl. (a-c) before immersion, (d-f) 2 days, (g-i) 20 days, (j-l) 70 days of immersion (carbon with orange, oxygen with purple, and zinc with yellow).

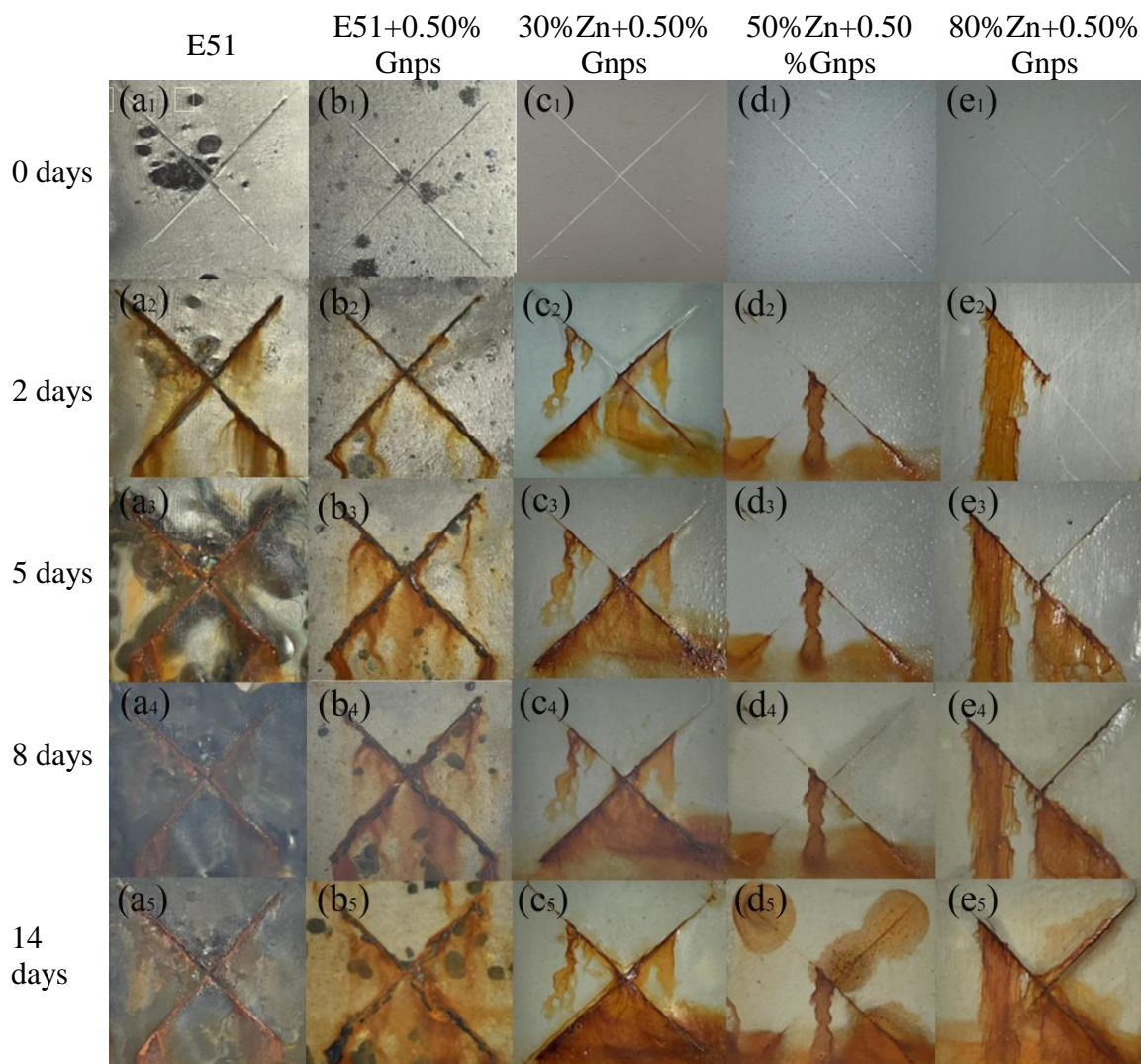
The EDS mapping spectra of the 50 % Zn+0.50 % Gnps coating at different immersion time were shown in

Figure . C, O, Zn elements were clearly detected in the coating. C, O elements came from epoxy resin. As seen from Fig. 8c, f, the spherical zinc particles disperse uniformly in the coatings before and after 2 days of immersion. The zinc particles near the metal base has not significantly reduced, indicating the metal has not undergone a large-scale corrosion. As mentioned, some holes remained after 20 days of immersion, and C, O elements showed a significant decreasing trend in Fig. 8g, h, it was due to the

elements can't be detected at the hole portion by using plane scanning. Meantime, a lower content of Zn element could be observed in Fig. 8i, indicating cathodic protection effect began to fail. The results may be due to the formation of a conductive network in the coatings by introducing highly conductive Gnps, leading to more and more isolated zinc particles which were uniformly corroded. After 70 days of immersion, the content of C, O, Zn elements continued to decrease in the coatings, indicating that the cathodic protection effect has completely failed.

#### 3.4. Salt spray test

The neutral salt spray images at different exposure times were shown in Fig. 9. Obviously, a great deal of rust appeared at the scratches on the E51 coating's surface after 2 days of salt spray testing in Fig. 9a<sub>1</sub>. Furthermore, it can be seen that the formation of black rusting on the substrate after 5 days of salt spray testing. As seen from Fig. 9b<sub>1</sub>, the width of rusting at the scratches became narrower after adding 0.50% Gnps, and the black rusting can't be observed on the substrate after 5 days of salt spray testing. It can be attributed to the physical shielding effect of Gnps, which can extend the diffusion path of the corrosive media to the carbon steel substrate, and result in the improvement of the coating's physical barrier. The E51 coating was completely penetrated with the extension of salt spray time in Fig. 9a<sub>3</sub>-a<sub>5</sub>, and the substrate was completely covered with black rust, while the E51+0.50% Gnps coating had a small part of black rust on the substrate in the same salt spray time. This illustrates that Gnps could enhance the corrosion resistance performance. Compared to the E51+0.50% Gnps coating, the coatings with three different zinc contents showed less red rust at the scratches in the same salt spray time. As seen from Fig. 9, there was a smaller area of red rust on the surface of the 50% Zn+0.50% Gnps and 80% Zn+0.50% Gnps coating than the 30% Zn+0.50% Gnps coating in the early stage. It can be attributed to the synergy between the high content of zinc particles and Gnps, resulting in excellent cathodic protection properties of the coatings. With time prolonged, the corrosion of the zinc-rich coatings progressed. There were blisters on the surface of the 30% Zn+0.50% Gnps coating after 5 days of salt spray testing in Fig. 9c<sub>3</sub>. As shown in Fig. 9c<sub>5</sub>, there were cracks on the surface of the 30% Zn+0.50% Gnps coatings after 14 days of salt spray testing, indicating that the cathodic protection effect has completely failed. The cracking can't be observed and has the smallest area of rust on the surface of the 50% Zn+0.50% Gnps coating in Fig. 9d<sub>2</sub>-d<sub>5</sub>, indicating that the coating has excellent anti-corrosion performance. The slight cracking was formed at the scratches of the 80% Zn+0.50% Gnps coating after 8 days of salt spray testing, meaning that the physical shielding effect is dominant at this moment. It can be concluded that the synergy between the high content of zinc particles and Gnps enhanced the cathodic protection ability and shielding effect of the coatings.



**Figure 9.** Images of the composite coatings after 14 days of salt spray testing. (a1-a5) E51, (b1-b5) E51+0.50 %Gnps, (c1-c5) 30 % Zn+0.50 % Gnps, (d1-d5) 50 % Zn+0.50 % Gnps, (e1-e5) 80 % Zn+0.50 % Gnps.

Water permeability resistance of epoxy coatings is closely related to epoxy coating protective performance. Generally, a higher WCA represents a more hydrophobic surface, thereby indicated the hydrophobic coating could effectively prevent the corrosion species permeating into the substrate [27]. Evolution of coating's water contact angle (WCA) during 14 days salt spray test was recorded in Fig. 10. Compared with E51 coating, the addition of 0.50 % Gnps increased the surface roughness of the coating and lead to the increase of contact angle value before salt spray testing [14]. As mentioned, the increase in contact angle could be attributed to the presence of defects for the zinc rich coating. With the salt spray time progressed, the contact angle exhibited a gradually increased trend for all coating. The reason was the coating surface severely damaged due to the corrosion solution diffusion and chloride ions attack. In addition, the significantly increased contact angle of the epoxy and 80 %Zn content coating could be observer in the early stage, indicated more surface damages appeared on the coating

and lead to the increase of surface roughness. Furthermore, the small contact angle fluctuations of 50 % Zn+0.50 % Gnps and 80 % Zn+0.50 % Gnps coating could be observed in Fig. 10 from 8 days to 14 days day. This phenomenon was associated with the surface roughness and the hydrophilicity of corrosion products [49].

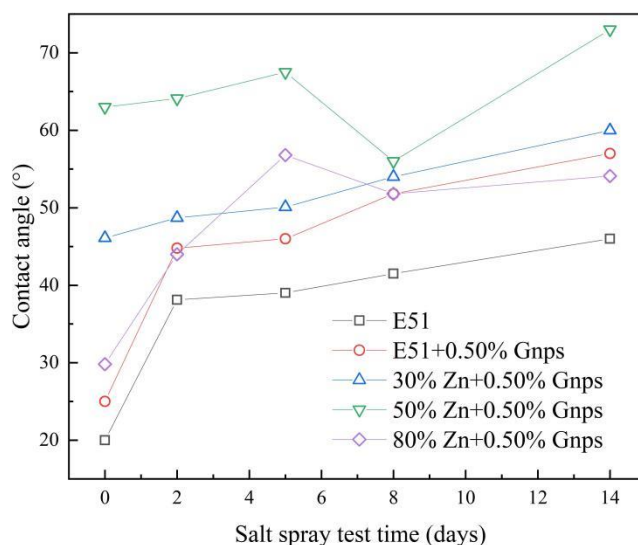


**Figure 10.** The contact angle of water on the coatings surface under different salt spray test time.

### 3.5. Corrosion protection mechanism

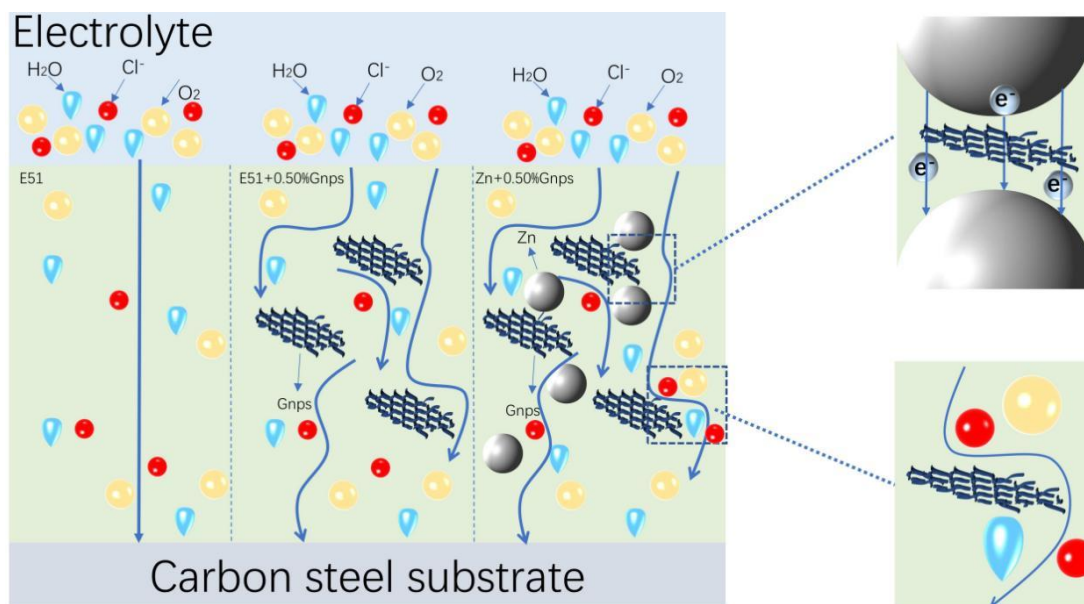


**Figure 11.** Schematic diagram of corrosion protection mechanism for different coatings.

Fig. 11 showed a diagram of the effect of Gnps and zinc power to the corrosion protection of epoxy resin. In terms of E51 coating, the corrosive media were easy to reach on the surface of steel substrate in the early stage, However, the addition of 0.50 % Gnps endowed the E51 coating with a better barrier effect due to increase the length of diffusion pathway. With the immersion time prolonged, these

two coatings formed a corrosion products layer which could seal the holes to maintain the stability of the corrosion protection performance for a period time. The barrier effect decreased significantly along with the corrosion products layer was penetrated by corrosion media in the later stage. The defects appeared in the 30 % Zn+0.50 % Gnps and 50 % Zn+0.50 % Gnps coating, this is caused by adding zinc particles, and the 0.50 % Gnps was not enough to improve the electrical connection of 30 % zinc content coating. Hence, the 30 % Zn+0.50 % Gnps exhibited a weak cathodic protection effect in the early stage. Conversely, powerful cathodic protection effect appeared in 50 % Zn+0.50 % Gnps coating which could be explained that more zinc particles been connected by Gnps to form electrically conductive network, thus provided a better excellent sacrificial anode protection for steel substrate. In addition, the cathodic protection period of 50 % Zn+0.50 % Gnps coating was longer than other coating samples, which might due to more zinc particles were activated as the time prolonged. Notably, the formation of zinc corrosion products could hold the anti-corrosion performance stable in the middle stage for 30 % Zn+0.50 % Gnps and 50 % Zn+0.50 % Gnps coating. In case of 80 % Zn+0.50 % Gnps coating, the holes were filled by a large amount of zinc corrosion products due to excellent cathodic protection in the early stage, this was explained that the Gnps was easy to improve the electrical connecting when 80 % zinc content was added. However, a relatively weaker corrosion protection effect than 50 % Zn+0.50 % Gnps coating was presented, indicated the zinc corrosion products wrapped up the unactivated zinc particles with the surrounding zinc powder were consumed. For all zinc rich coatings, the barrier effect of corrosion products and Gnps took a dominant position when the cathodic protection performance failed.

#### 4. CONCLUSIONS

The EIS measurement, salt spray test, contact angle, SEM, EDS were employed to study the synergy effect between zinc particles and Gnps to the corrosion protection performance of epoxy resin coating. The conclusion are as follows:

(1) It was found that the epoxy coating modified by 0.50 % Gnps enhanced the improvement of barrier performance. The high zinc content coating had a better electrical connection and cathodic protection effect than low zinc content coating when the 0.50 % Gnps was added.

(2) The 30 % Zn+0.50 % Gnps coating presented a mixed corrosion protection mechanism of shielding and cathodic protection during the whole immersion test. For 50 % Zn+0.50 % Gnps and 80 % Zn+0.50 % Gnps coating, the excellent cathodic protection and barrier effect took a dominant position in the early and later stage, respectively.

(3) Based on EIS, salt spray, contact angle, SEM, and EDS, it is indicated that the addition of 0.50 % Gnps possessed the most significant strengthening effect on the 50 % zinc content coating, followed by 80 % Zinc content coating. And the worst was 30% zinc content and epoxy coating. This demonstrated the addition of 0.50 % Gnps could lower the concentration of zinc particles in the coating. This study may expand the application of Gnps in the field of anti-corrosion coating.

## ACKNOWLEDGEMENTS

The authors would like to acknowledge Prof. Hu Wang for his contribution in proofing reading the article. This research did not receive any specific grant from funding agencies in the public, commercial, or not-for-profit sectors.

## References

1. Y.J. He, I. Dobryden, J.S. Pan, A. Ahniyaz, T. Deltin, R.W. Corkery and P.M. Claesson, *Appl. Surf. Sci.*, 457 (2018) 548.
2. A.A. Javidparvar, R. Naderi and B. Ramezanzadeh, *Composites, Part B*, 172 (2019) 363.
3. Z. Mahidashti, T. Shahrabi and B. Ramezanzadeh, *Prog. Org. Coat.*, 114 (2018) 19.
4. D.W. Zhang, H.C. Qian, L.T. Wang and X.G. Li, *Corros. Sci.*, 103 (2016) 230.
5. L. S, W.J. Zhao and L.J. Miao, *J. Hazard. Mater.*, 403 (2021) e123670.
6. K. Schaefer and A. Miszczyk, *Corros. Sci.*, 66 (2013) 380.
7. L.H. Cheng, C.L. Liu, D.J. Han, S.H. Ma, W.H. Guo, H.F. Cai and X.H. Wang, *J. Alloys Compd.*, 774 (2019) 255.
8. A. Gergely, E. Pfeifer, I. Bertoti, T. Torok and E. Kalman, *Corros. Sci.*, 53 (2011) 3486.
9. L. Shen, Y. Li, W.H. Zhao, L.J. Miao, W.P. Xie, H.M. Lu and K. Wang, *ACS Appl. Nano Mater.*, 2 (2019) 180.
10. H. Hayatdavoudi and M. Rahsepar, *J. Alloys Compd.*, 727 (2017) 1148.
11. S. Park and M. Shon, *J. Ind. Eng. Chem.*, 21 (2015) 1258.
12. S.Y. Arman, B. Ramezanzadeh, S. Farghadani, M. Mehdipour and A. Rajabi, *Corros. Sci.*, 77 (2013) 118.
13. T.H. Ge, W.J. Zhao, X.D. Wu, X.J. Lan, Y.G. Zhang, Y.J. Qiang and Y.L. He, *J. Colloid Interface Sci.*, 567 (2020) 113.
14. N.N. Taheri, B. Ramezanzadeh and M. Mahdavian, *J. Alloys Compd.*, 800 (2019) 532.
15. R. Ding, S. Chen, J. Lv, W. Zhang, X.D. Zhao, J. Liu, X. Wang, T.J. Gui, B.J. Li, Y.Z. Tang and W.H. Li, *J. Alloys Compd.*, 806 (2019) 611.
16. R. Ding, Y. Zheng, H.B. Yu, W.H. Li, X. Wang and T.J. Gui, *J. Alloys Compd.*, 748 (2018) 481.
17. S. Teng, Y. Gao, F.L. Cao, D.B. Kong, X.Y. Zheng, X.M. Ma and L.J. Zhi, *Prog. Org. Coat.*, 123 (2018) 185.
18. S.R. Wang, J.W. Yang, J.P. Cao, L.J. Gao and C.X. Yan, *Int. J. Electrochem. Sci.*, 14 (2019) 9671.
19. J.R. Liu, T. Liu, Z.W. Guo, N. Guo, Y.H. Lei, X.T. Chang and Y.S. Yin, *Polym.*, 10 (2018) e591.
20. S.Y. Huang, G. Kong, B. Yang, S.H. Zhang and C.S. Che, *Prog. Org. Coat.*, 140 (2020) e105531.
21. X.Y. Wang, A. Narita and M. Klaus, *Nat. Rev. Chem.*, 2 (2018) e0100.
22. S. Farah, A. Farkas, J. Madarasz and K. Laszlo, *J. Therm. Anal. Calorim.*, 142 (2020) 331.
23. O. Akhavan, *Carbon*, 48 (2010) 509.
24. GB/T 1771-2007 (Paints and varnishes-Determination of resistance to neutral salt spray) Standards.
25. A. Kaniyoor and S. Ramaprabhu, *Aip Adv.*, 2 (2012) e032183.
26. G. Calderon-Ayala, M. Cortez-Valadez, M. Acosta-Elias, P.G. Mani-Gonzalez, M.E. Zayas, S.J. Castillo and M. Flores-Acosta, *J. Electron. Mater.*, 48 (2019) 1553.
27. S.G. Zhou, Y.M. Wu, W.J. Zhao, J.J. Yu, F.W. Jiang, Y.H. Wu and L.Q. Ma, *Mater. Des.*, 169 (2019) e107694.
28. F.W. Jiang, W.J. Zhao, Y.M. Wu, Y.H. Wu, G. Liu, J.D. Dong and K.H. Zhou, *Appl. Surf. Sci.*, 479 (2019) 963.
29. Y. Wang, Y.B. Ma, G.Z. Guo, Y.Y. Zhou, Y.Y. Zhang, Y.Y. Sun and Y.Q. Liu, *Int. J. Electrochem. Sci.*, 12 (2017) 2135.
30. E.M.A. Martini and I.L. Muller, *Corros. Sci.*, 42 (2000) 443.
31. H. Li, J.B. Pu and R.H. Zhang, *Surf. Topogr. Metrol. Prop.*, 7 (2019) e045022.
32. T.H. Ge, W.H. Zhao, X.D. Wu, L. Shen, X.J. Ci and Y.L. He, *J. Hazard. Mater.*, 186 (2020)

- e108299.
33. Y. Tian, Z.X. Bi and G. Cui, *polym.*, 13 (2021) e1657.
  34. R. Mohammadkhani, M. Ramezanzadeh, S. Saadatmandi and B. Ramezanzadeh, *Chem. Eng. J.*, 382 (2020) e122819.
  35. M.Y. Rekha and C. Srivastava, *Corros. Sci.*, 152 (2019) 234.
  36. F. Rosalbino, G. Scaviho, D. Maccio and A. Saccone, *Corros. Sci.*, 89 (2014) 286.
  37. M. Mahdavian and M.M. Attar, *Corros. Sci.*, 48 (2006) 4152.
  38. X. Wang, S. Chen, R. Ding, N. Zhou, Y. Zheng, H.B. Yu, B.J. Li, T.J. Gui and W.H. Li, *Int. J. Electrochem. Sci.*, 14 (2019) e3553.
  39. X. Cao, F. Huang, C. Huang, J. Liu and Y.F. Cheng, *Corros. Sci.*, 159 (2019) 108.
  40. X. Wang, X.F. Zhang, E.B. Caldona, W.Q. Leng, J. Street, G.P. Wang and Z. Zhang, *J. Environ. Chem. Eng.*, 9 (2021) e105707.
  41. Z.W. Song and B. Qian, *Mater. Corros.*, 69 (2018) 1854.
  42. X.M. Luo, H.R. Yin, J. Ren, H.P. Yan, X. Huang, D.H. Yang and L.M. He, *J. Colloid Interface Sci.*, 545 (2019) 35.
  43. S. Shreepathi, P. Bajaj and B.P. Mallik, *Electrochim. Acta*, 55 (2010) 5129.
  44. M. Zubielewicz, E. Langer, A. Krolkowska, L. Komorowski, M. Wanner, K. Krawczyk, L. Aktas and M. Hilt, *Prog. Org. Coat.*, 161 (2021) e106471.
  45. W.C. Bai, Y.T. Ma, M.J. Meng and Y. Li, *Prog. Org. Coat.*, 161 (2021) e106456.
  46. P. Mahato, S.K. Mishra, M. Murmu, N.C. Murmu, H. Hirani and P. Banerjee, *Surf. Coat. Technol.*, 375 (2019) 477.
  47. M. Murmu, S.K. Saha, N.C. Murmu and P. Banerjee, *J. Mol. Liq.*, 278 (2019) 521.
  48. M. Murmu, S.K. Saha, N.C. Murmu and P. Banerjee, *Corros. Sci.*, 146 (2019) 134.
  49. C.L. Zhang, Y. He, Z.H. Xu, H. Shi, H.H. Di, Y. Pan and W. Xu, *Polym. Adv. Technol.*, 27 (2016) 740.